

Hematological and Vascular Defects in a Model of Null and Type 2B VHL Mutations

Background

Von Hippel-Lindau (VHL) syndrome is an autosomal dominant predisposition to numerous types of highly vascular tumors dispersed across multiple organ systems. VHL syndrome principally involves dysregulation of oxygen sensing pathways including the Hypoxia Inducible Factor (HIF)-Vascular Endothelial Growth Factor-A (VEGF-A) and HIF-Erythropoietin (EPO) signaling axes. Previous work by our lab identified vascular morphological changes and transcriptional aberrations unique to functional VHL loss scenarios in the developmental time period. Additionally, our lab observed a unique, erythematous, phenotype unique to post-developmental tamoxifen exposure in the setting of inducible Cre-recombinase-mediated VHL loss or 2B mutation. In order to extend our VHL model towards a more clinically relevant scenario (i.e. correlating to an early adulthood 'second-hit') and to explore the molecular and morphological underpinnings of this phenotype, we developed a post-developmental VHL excision model. Our hypotheses for this erythematous phenotype included changes in red blood cell density downstream of HIF-EPO-JAK2 signaling and/or vascular morphology changes with increased arteriogenic remodeling downstream of VEGF-A and Notch pathways. We further hypothesized that vascular flow perturbations related to blood viscosity changes might drive vascular remodeling as well as changes to vessel permeability, potentially mediated by changes in expression of Claudin5 (*Cldn5*), a tight junction molecule critical for vessel barrier function. This idea aligns with data published in Arreola et al. 2018 in which we found preliminary evidence for downregulated *Cldn5* expression in the setting of VHL loss (null) and 2B mutation within our developmental model.

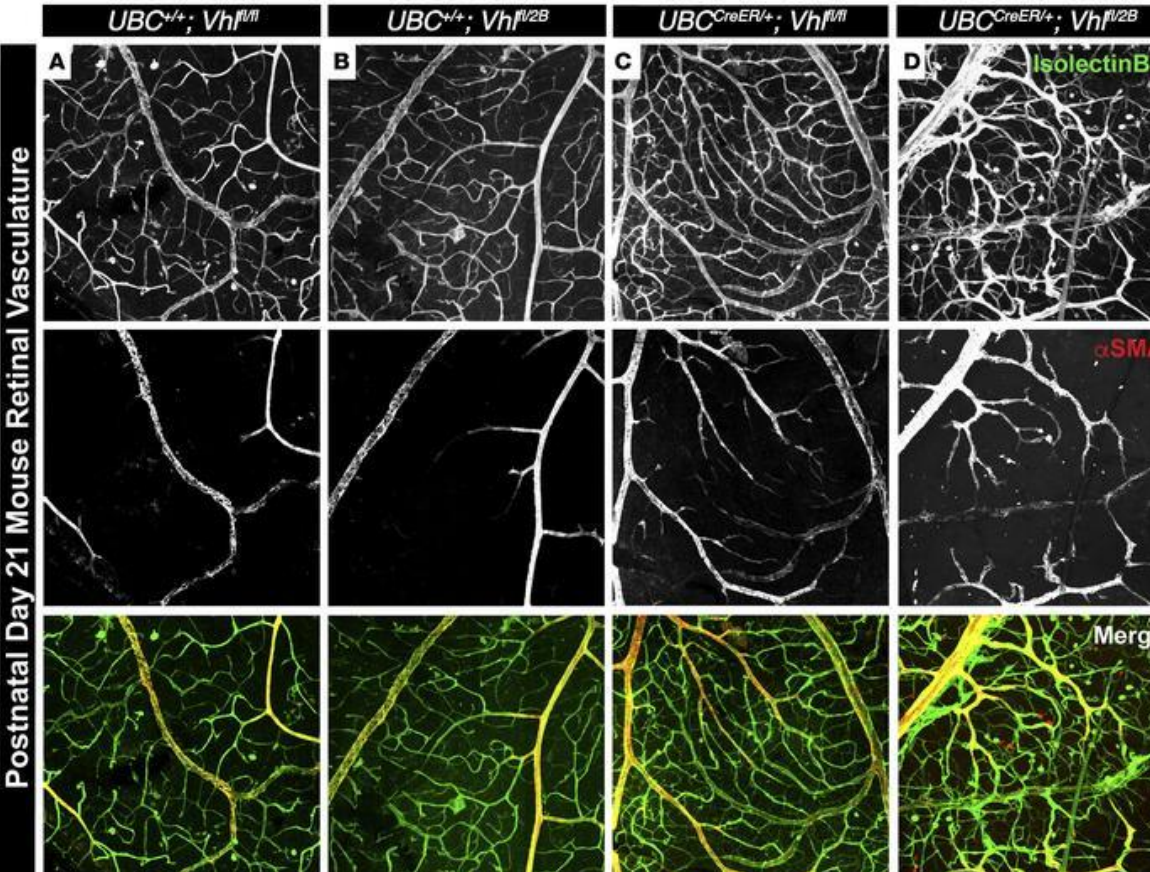


Fig 1. Retinal Vasculature in Developing VHL Mutants from Arreola et al. JCI Insight 2018.

phenotype unique to post-developmental tamoxifen exposure in the setting of inducible Cre-recombinase-mediated VHL loss or 2B mutation. In order to extend our VHL model towards a more clinically relevant scenario (i.e. correlating to an early adulthood 'second-hit') and to explore the molecular and morphological underpinnings of this phenotype, we developed a post-developmental VHL excision model. Our hypotheses for this erythematous phenotype included changes in red blood cell density downstream of HIF-EPO-JAK2 signaling and/or vascular morphology changes with increased arteriogenic remodeling downstream of VEGF-A and Notch pathways. We further hypothesized that vascular flow perturbations related to blood viscosity changes might drive vascular remodeling as well as changes to vessel permeability, potentially mediated by changes in expression of Claudin5 (*Cldn5*), a tight junction molecule critical for vessel barrier function. This idea aligns with data published in Arreola et al. 2018 in which we found preliminary evidence for downregulated *Cldn5* expression in the setting of VHL loss (null) and 2B mutation within our developmental model.

Methods

Tamoxifen induced Cre-recombinase excision of floxed VHL alleles was performed at postnatal day 28 (P28), one week post-weaning. Additional experiments involved injections at the 11-15 month time point and adult breeders with second-hand tamoxifen exposure from pups.

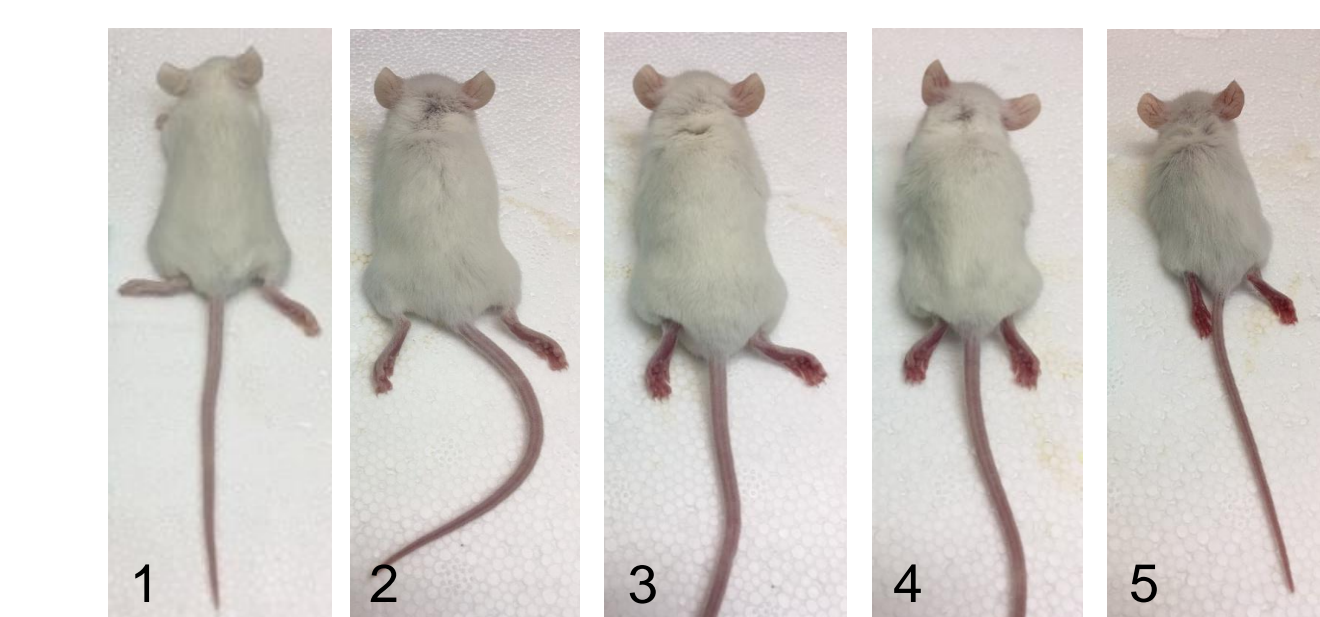
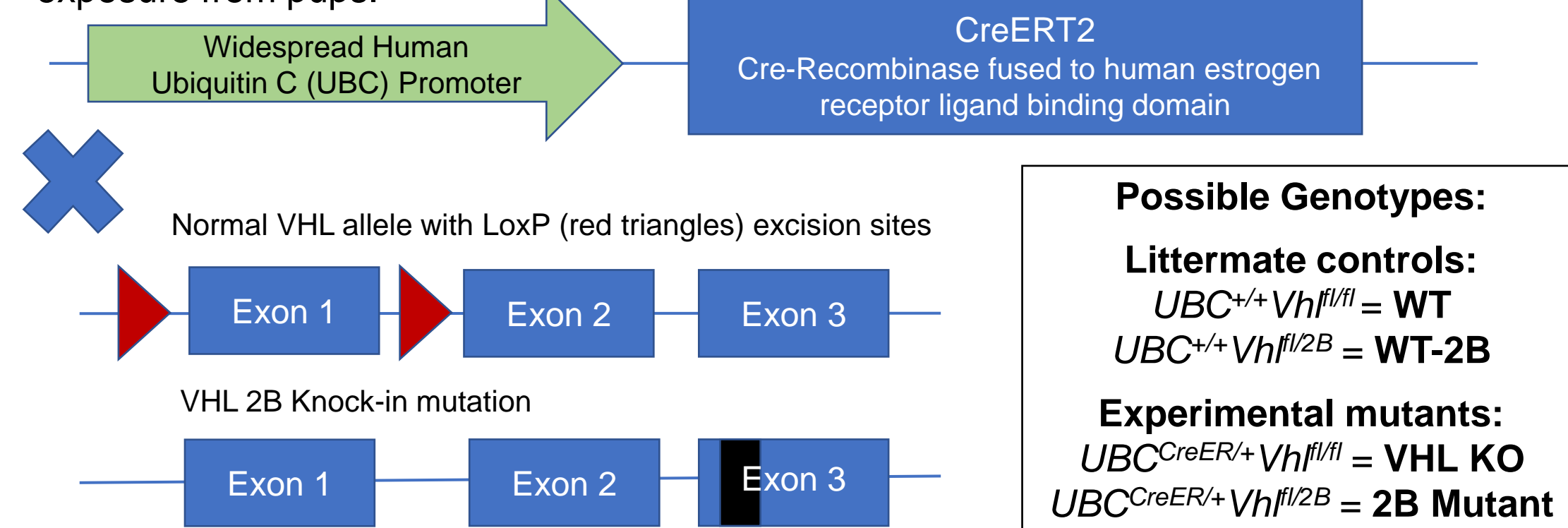


Fig 2. Animals were assigned redness scores from 1-5 based on comparative grading of ear, foot, tail, and visceral organ erythema, and the presence or absence of visible ear vessels.

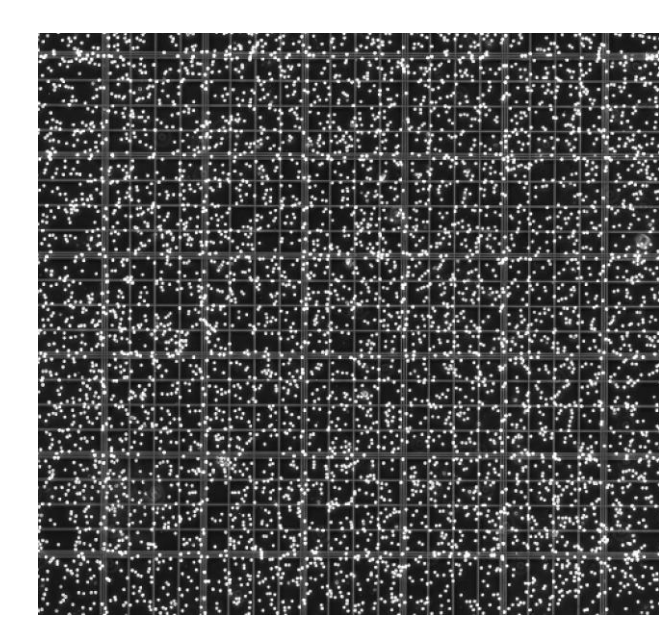


Fig 3. Red blood cells were imaged on a hemocytometer and quantified immediately post-mortem.

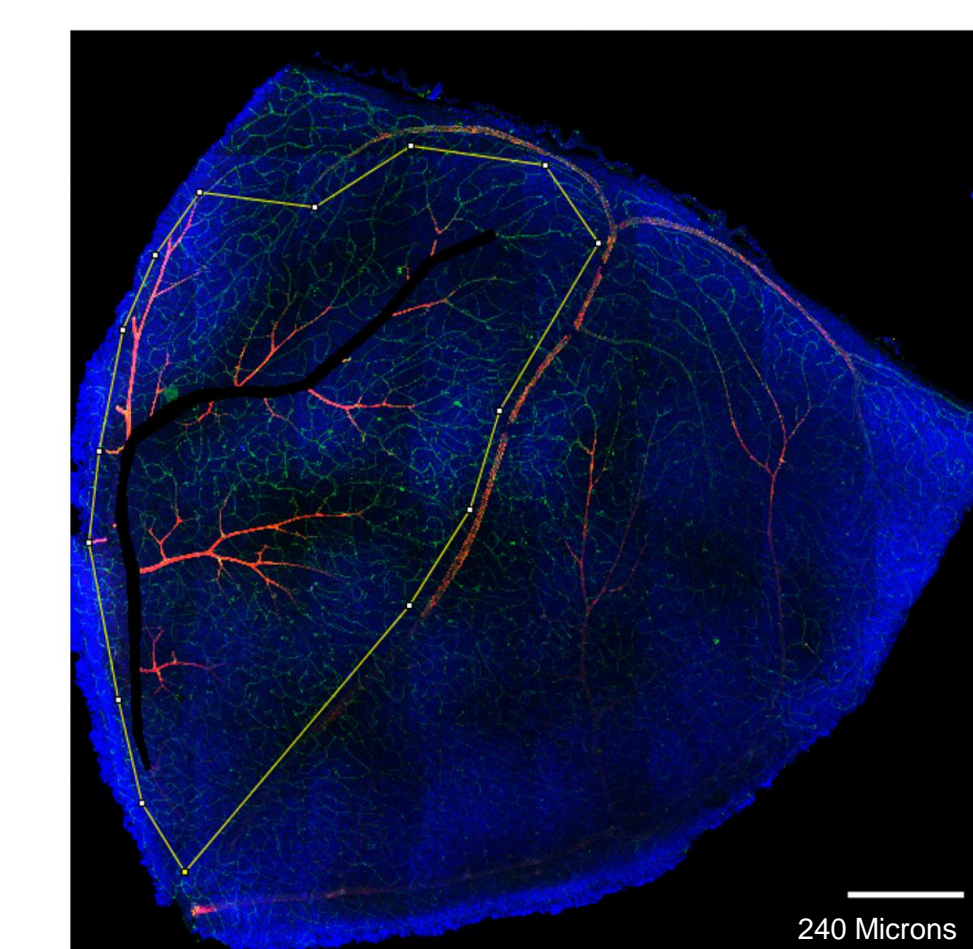
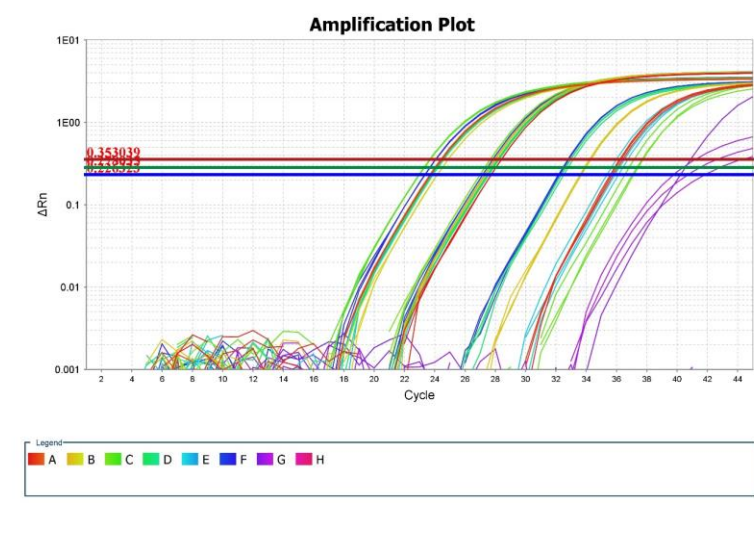


Fig 4. Whole retinas were harvested, fixed, and micro-dissected into leaflets, which were immunostained with the following antibody combinations: IsolectinB4 to visualize endothelial cells (green), Cy3-conjugated anti-aSMA to visualize smooth muscle cells (red), anti-NG2 to visualize pericytes (not shown), and DAPI to visualize cell nuclei (blue). 20x tile scans were obtained using a Zeiss LSM 880 confocal microscope. Images were analyzed using ImageJ software to determine aSMA coverage within distal arterial vascular beds, excluding the main feeding artery, consistent with our previous analysis in Arreola et al. 2018.

Fig 5. Representative amplification plot for P28 injected and adult breeder experimental kidney samples that were homogenized and processed for mRNA purification and qRT-PCR analysis using the TaqMan® system. Genes analyzed: Mouse *Ldha*, *Epo*, and *Tbp* (endogenous control). R software was used for statistical analysis for this experiment and all experiments described above.



Results

Smooth Muscle α-Actin (aSMA) Coverage Excluding Main Artery

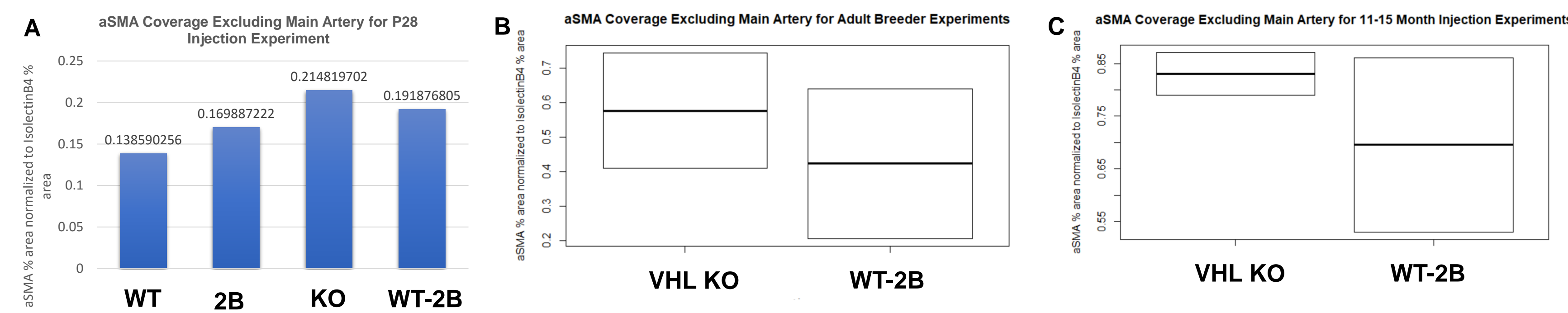


Fig 6. A: P28 retinas measured for aSMA coverage of distal arteries excluding primary feeder vessel. No statistics computed for P28 experiments. B: Adult VHL breeders indirectly exposed to tamoxifen. Two-tailed Student's t-test found no significant difference in mean aSMA/IsolectinB4 ratio between CRE positive and negative adult breeder experimental samples ($p = 0.63$). C: Tamoxifen-injected 11-15 month adults. Two-tailed Student's t-test found no significant differences in the mean aSMA/IsolectinB4 ratios between CRE positive and negative 11-15 month injection experimental samples ($p = 0.51$). Note: Due to COVID-19 quarantine orders, sample sizes have thus far been limited to $n=1$ for all genotypes in P28 experiment, and $n=2$ for both genotypes in adult breeder and 11-15 month injection experiments.

Representative Images

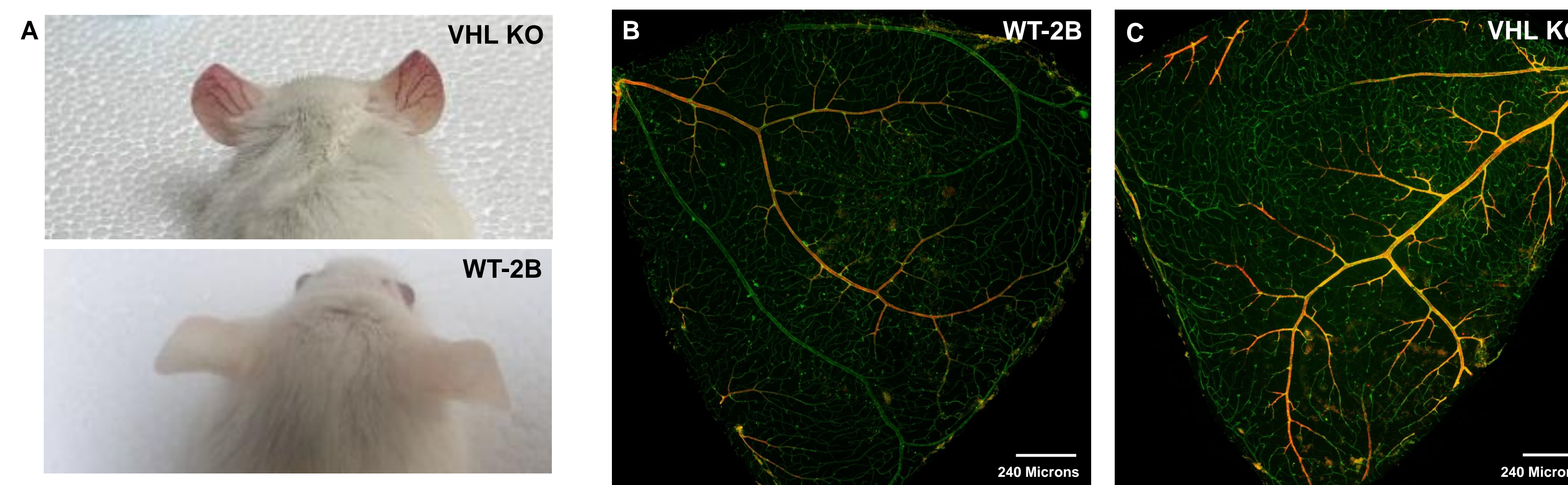


Fig 7. A: Top – redness score = 5 (VHL KO adult breeder sample); Bottom – Redness score = 1 (WT-2B adult breeder sample). B: 20x tile scan of CRE negative adult breeder immunostained retina (red channel corresponding to aSMA, green channel corresponding to Isolectin-B4). C: 20x tile scan of CRE positive adult breeder immunostained retina (red channel corresponding to aSMA, green channel corresponding to Isolectin-B4). Panels B and C are representative images illustrating observed increase in aSMA coverage distal to the main artery in the setting of *Vhl* dysfunction.

Epo and Ldh-a Gene Expression Changes

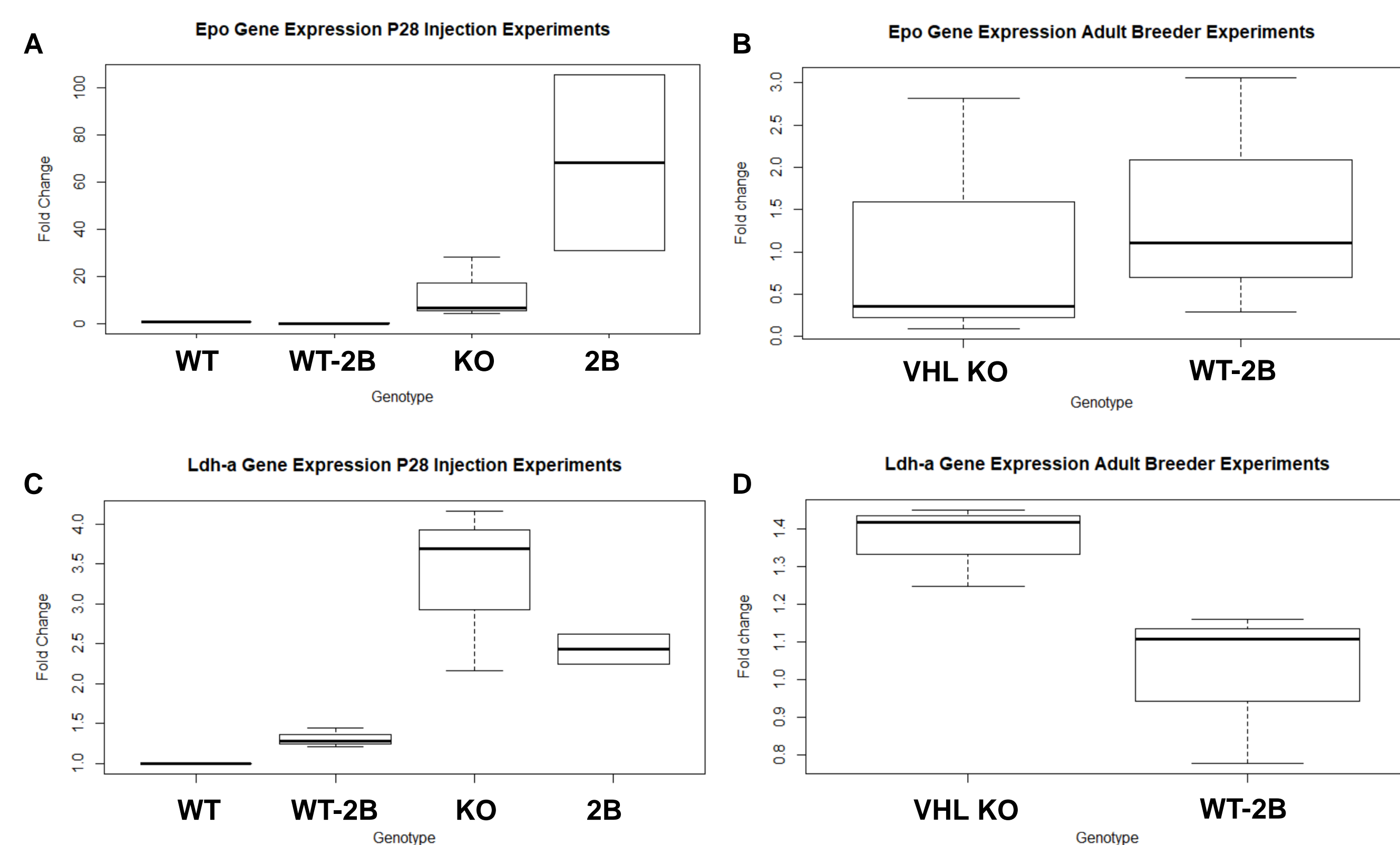


Fig 8. *Epo* and *Ldh-a* gene expression changes were experimentally determined with P28 and adult breeder experimental samples, using *Tbp* as an endogenous control gene. Average fold change and statistics were computed for P28 and adult breeder experiments individually. One-way ANOVA and Student's two-tailed t-test for P28 experiments and adult breeder experiments, respectively, did not identify significant differences in *Epo* and *Ldh-a* gene expression in all cases. A: $p = 0.112$, B: $p = 0.76$, C: $p = 0.045$ (post-hoc analysis revealed most significant source of variation to be 0.05), D: $p = 0.06$. In most cases, a trend was evident for increased *Epo* and *Ldh-a* expression in *VHL* loss scenarios; however a paradoxical downregulation of *Epo* was evident for CRE positive adult breeders.

Erythema Scoring & Red Blood Cell Count

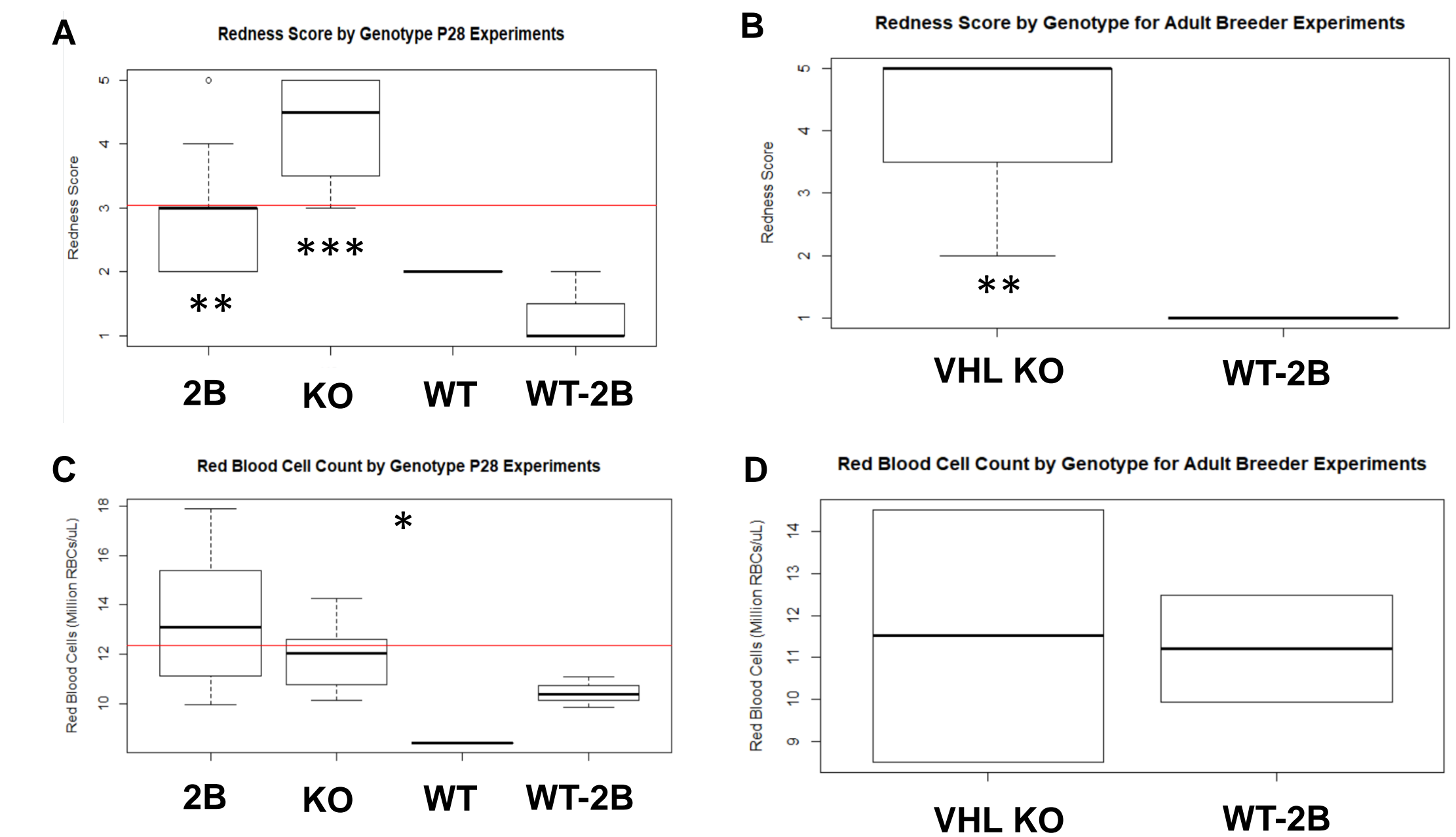


Fig 9. A: Redness Score in P28 experiment ($p < 0.001$). Post-hoc analysis revealed significant difference between KO and 2B mutant ($**p = 0.006$), WT2B and 2B mutant ($**p = 0.007$), and WT2B and KO ($***p = 0.00002$). B: Redness score between the CRE-positive and -negative adult breeders ($**p = 0.04$). C: RBC density across genotypes; significant differences found, however the source of variation was unable to be determined, likely due to $n=1$ in WT group. D: No significant difference in mean RBC count between CRE positive and negative adult breeders ($p = 0.93$).

Claudin-5

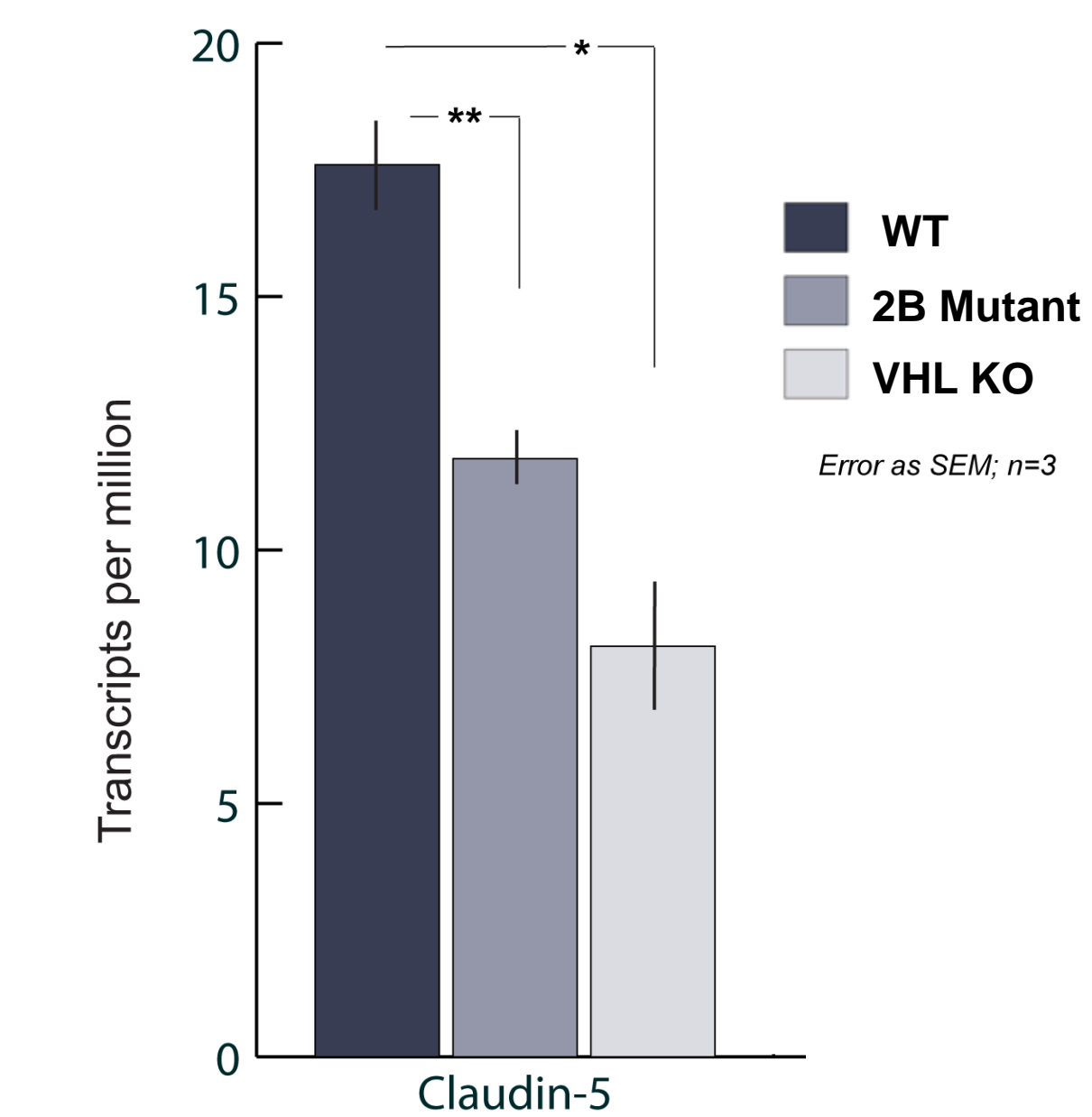


Fig 10. RNA-Seq data from Arreola et al. JCI Insight 2018 suggesting Claudin-5 downregulation proportionate to the degree of *Vhl* dysfunction (greater downregulation in the induced VHL KO scenario than in the Type 2B mutants).

This observation, together with the observations from current early adult (P28) experiments (presumed increased blood viscosity and arterIALIZATION with *Vhl* loss-of-function) indicate a potential relationship between Claudin-5, a tight junction protein, and the interplay between blood flow dynamics and vascular remodeling.

Conclusions and Future Directions

- Vhl* status and age at 'second-hit' may uniquely affect downstream pathways crucial to hematologic and vascular homeostasis.
- The observed erythematous phenotype is likely multifactorial in etiology, dependent on functional *Vhl* status and timeline of disease presentation.
- Extrapolating the above conclusion-- disease pathology in the human condition may also be mutation- and timeline-specific; thus, pharmacologic interventions should be tailored to specific phenotypic and molecular presentations unique to each patient, when possible.
- Changes in blood viscosity and vessel morphology may have specific effects on blood flow. These effects may impact tumor progression and drug delivery, and therefore must be further examined for the impact on the disease state and therapeutic interventions.
- Unique abnormalities in blood viscosity and flow may imply risk for certain complications in the setting of *Vhl* loss or mutation (e.g. hyper-viscosity syndrome and thrombotic events).
- Claudin-5 may be an effector of structural remodeling within vascular networks responding to the blood flow perturbations caused by *Vhl* loss-of-function and/or mutation.
- In the current study, more replicates will be needed, and in general more research must be done to translate the relevance of these findings from the animal model to the bedside.

Acknowledgements

Thank you to the Fralin Biomedical Research Institute at Virginia Tech-Carilion and Virginia Tech Carilion School of Medicine for institutional support.

Vhl:G518A mouse line acquired from Rathmell Lab, Vanderbilt Univ.

NIH – R01HL146596 (to J.C.C.)
AHA – 19TPA34910121 (to J.C.C.)
NSF CAREER Award – 1752339 (to J.C.C.)